

Variation of Conductivity of Fullerite Structures Under Different Types of Pressure

A.S. Berdinsky, D. Fink*, Hui-Gon Chun**[†], Yong-Zoo Yoo**, Ji-Beom Yoo***,
A.V. Petrov*, and P.S. Alegaonkar****

Abstract

It is known that the conductivity of fullerite depends on the applied pressure. In this paper we compare the variation of conductivity of three different fullerite structure with pressure. We examined C₆₀ powder, filled into thin glass capillaries and also studied fullerite nanotubules produced within etched swift heavy ion tracks in polymer foils. These investigations are compared with the results of planar Si-C₆₀-Au structures.

Key Words : fullerite, powder, tubules, thin films, ion tracks, polymer foils, pressure, conductivity

1. Introduction

The crystalline state of fullerene C₆₀, called fullerite, is a semiconductor with wide band gap E_g of about 1.7 – 1.9 eV, Ref.^[1]. The type of bond between C₆₀ molecules in fullerite crystal is based on van der Waals interaction. This means that the compressibility of fullerite under hydrostatic pressure is very high and resistance of fullerite has to change dramatically as result of applied pressure. As it had been shown recently in Ref.^[2] the conductivity was changed from $10^{-6} - 10^{-7} \Omega^{-1} \cdot \text{cm}^{-1}$ at normal pressure to $5 \Omega^{-1} \cdot \text{cm}^{-1}$ under pressure from 100 to 200 kbar. The changes in conductivity are concerned with variation of the crystal volume as a result of hydrostatic compression. For fcc lattice of fullerite isothermal bulk modulus is $K_0 = 18.1 \pm 1.8$ GPa and $dK_0/dP = 5.7 \pm 0.6$. This means the relative variation of the crystal volume exceeds 30% at 200 kbar^[3]. Thus fullerite appears the properties of sensitive material to pressure hence it could be considered as prospective material for pressure sensors.

In principal, fullerene can be used as functional mate-

rial for electronic device or sensors as individual molecule^[4] or in solid modification, e.g. crystalline form^[5], polycrystalline film^[6-8] and powder^[9]. Fullerene solids differ from conventional electronic materials because the fullerene molecule is the fundamental building block of the crystalline phase. Unique features about fullerenes include the structural perfection and reproducibility of these subnanometer building blocks^[1]. The application fullerite, for the creation of the sensors of light, temperature, humidity and pressure has been discussed^[8,10-12]. The first studies have shown, however, that the technical realization is not that easy, but the measured properties depend, to some extent, on the structure of the used fullerite.

The using of fullerite as wide-band gap semiconductor which performs n-type of conductivity^[7] in different construction of sensors allows to apply axial or isotropic pressure. Therefore, in this work, the investigations of pressure dependence of the fullerite conductivity of differently assembled C₆₀ structures have been made.

2. Experimental

In the first case, C₆₀/C₇₀ powder (weight ratio 85:15) was filled into glass capillaries of 1.5 and 0.75 mm diameter. The powder with a grain size of typically 30 – 40 μm has been synthesized, as usual, by arc discharge and subsequent chromatographic cleaning. The powder in the column was compressed by two metals, which also served as electrical contacts, Fig. 1a. In the

Novosibirsk State Technical University, K. Marx Ave. 20, 630092, Novosibirsk, Russia

*Hahn-Meitner-Institut, Glienicke Str. 100, D-14109, Berlin, Germany
**ReMM, School of Materials Science and Engineering, University of Ulsan, Korea

***Dept. of Materials Engineering, Sungkyunkwan University, Korea

****Dept. of Physics, University of Pune, India

[†]Corresponding author: hgchun@mail.ulsan.ac.kr

(Received : August 1, 2003, Accepted : July 16, 2004)

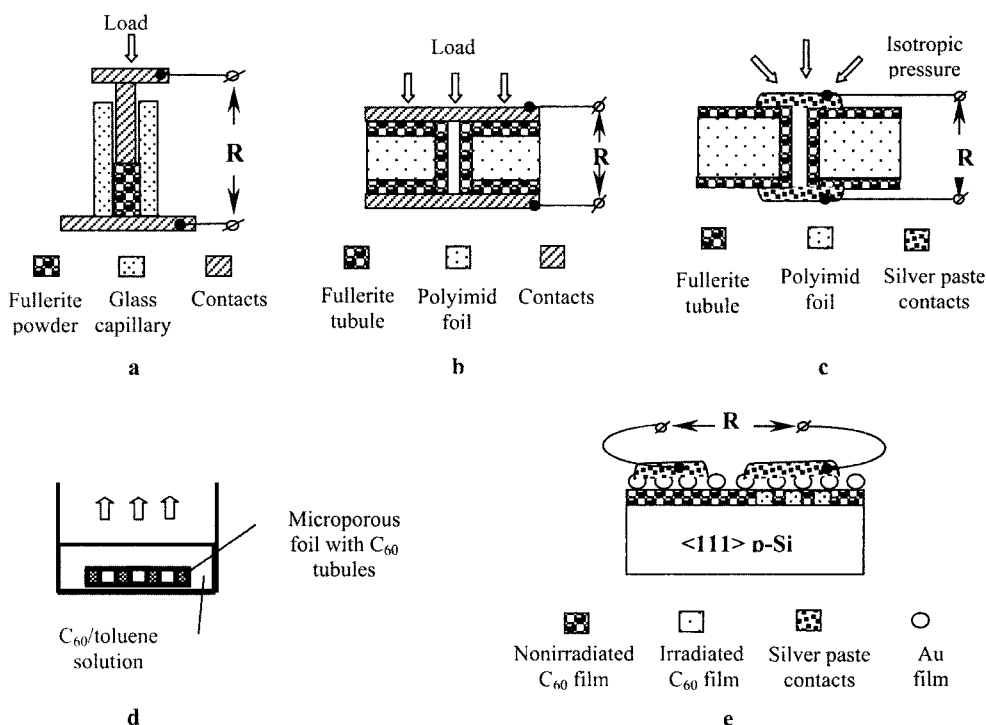


Fig. 1. Experimental arrangements used in this work. Set-up for measurement of electrical resistance of fullerite: a) unidirectional compression of C_{60} powder [1 bottom plane contact (silver); 2 upper-rod contact (copper)], b) unidirectional, c) isotropic compression of C_{60} tubules, d) principle sketch of tubule formation, and e) for comparison, the experimental arrangement of [2] for the determination of the isotropic compression of evaporated pristine and ion-irradiated fullerite films.

second case, pure C_{60} or C_{60}/C_{70} (85:15) tubules were formed within etched tracks in PI or PET foils. The nanopores were formed by perpendicular irradiation of the polymer foils with a beam of 300 MeV $^{86}\text{Kr}^{14+}$ ions at a fluence of 10^9 cm^{-2} . Subsequent etching with 3 mol/l NaOCl removed a nearly cylindrical zone of about 0.2 to 5 μm diameter along the ion track axis. After washing dried foil samples were put into a saturated C_{60} /toluene solution, Fig. 1b. During the complete evaporation of the solvent the over saturated fullerite precipitated heterogeneously on all available solid walls - i.e. on the walls of the vessel, foil surface, and on the inner walls of the etched tracks. This process was repeated several times to obtain C_{60} tubules with different wall thickness. The latter ones were derived from the differences of the inner fullerite tubule radii and the original etched track radius, as determined by the Ion Transmission Spectrometry^[13]. From Fig. 3 one can see also the cross-sectional area of fullerite tubule. SEM images of the

obtained structures are presented in Fig. 4. PI foils with embedded C_{60} tubules with 250 nm wall thickness (corresponding to 15 deposition steps, see Fig. 2) were then exposed to different loads, Fig. 1b.

On the other hand, PET samples with fullerite tubules of 20 nm thickness (corresponding to the deposition of one layer only) were exposed to different pressures at ambient air and dry nitrogen atmospheres, Fig. 1c. A PI sample was then embedded within 2 glass plates onto which chromium electrodes had been evaporated before, Fig. 1b. The PET samples were covered by conducting Ag paste on both sides to establish electrical contacts, Fig. 1c.

These experiments are compared with earlier ones. Here, we had examined planar 250 nm thick C_{60} films evaporated onto a $\langle 111 \rangle$ oriented p-Si wafer, onto which a 5 nm thick Au layer had been vapor-deposited. After ageing for several years the badly wetting Au films crack so that intermittent, small metal platelets emerge on the C_{60} base layer, Fig. 1e. Those samples

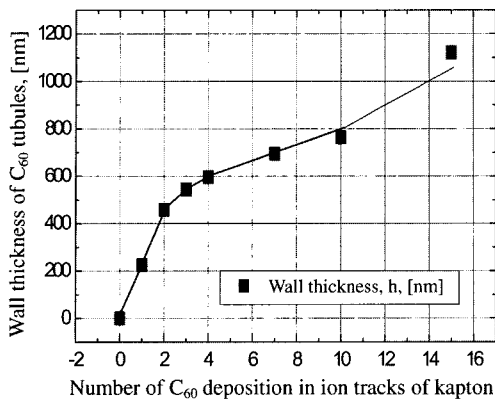


Fig. 2. Wall thickness of the C₆₀ fullerite tubules in etched ion tracks in correlation with to the number of deposition steps.

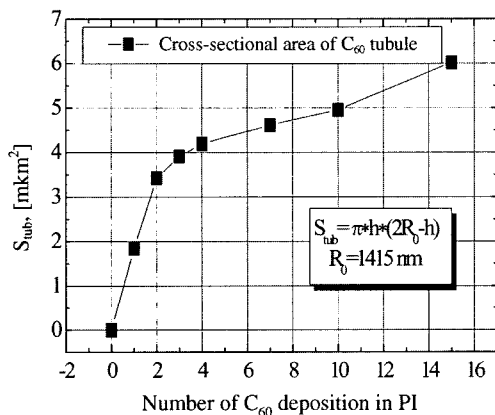


Fig. 3. Cross-sectional area of C₆₀ tubule in kapton as function of deposition number.

enable one to measure the surface conductance through the fullerite film, as the laterally non-conducting Au coverage does not shortcut the currents through C₆₀. These samples had partly been irradiated with 300 MeV ⁸⁴Kr¹⁴⁺ ions to probe additionally the influence of irradiation damage. The influence of isotropic pressure of the surrounding ambient air was also studied in this case.

3. Results and Discussion

The Fig. 5 shows the principal results of these measurements. The quantitative estimation of the results could be made by the factor of pressure sensitivity has been found by the following expression:

$$S = \frac{R(P_0) - R(P_x)}{R(P_0) \cdot \Delta P}, Pa^{-1}, \text{ where } R(P_0) \text{ and } R(P_x) \text{ are}$$

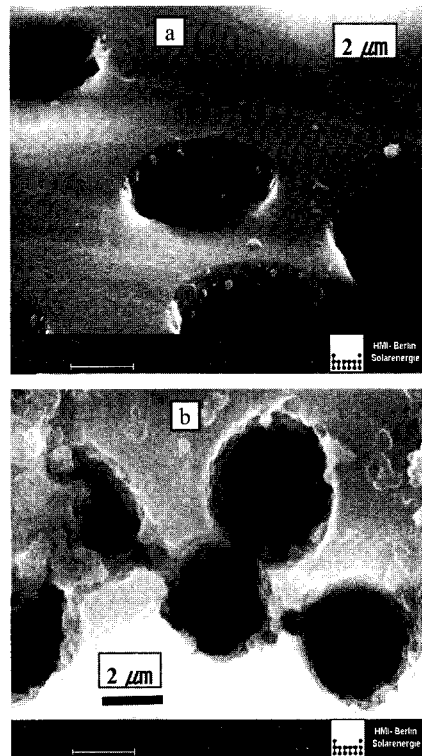


Fig. 4. SEM images of C₆₀ tubules in etched ion tracks in polyimide; a) PI foil covered with 5 C₆₀ layers. Please note the extraordinary smoothness of the overall sample surface if the deposited C₆₀ films are kept thin enough. Additionally, some film fragments and small clusters are seen on the surfaces and b) PI foil covered with 15 C₆₀ layers. Though a major part of the foil surface is still rather smooth, some additional flakes are seen to cover other surface regions, and pronounced nanocrystal growth is seen to start within the etched track walls.

the resistances at initial, P_0 , and final, P_x , points of pressure range; $\Delta P = P_x - P_0$ is pressure difference.

The main feature of pressure dependences of resistance $R(P)$, see Fig. 5a, b, c, d, e, is appearance of two different branches with strong and non-linear dependence of $R(P)$, which can be described by the factor of pressure sensitivity (S_1), and weak and quasi-linear dependence of $R(P)$, which can be described by the factor of pressure sensitivity (S_2), respectively. These parts of $R(P)$ curves correspond to low pressure branch, (S_1), and high pressure branch, (S_2).

We think that in the case of powder composition (Fig.

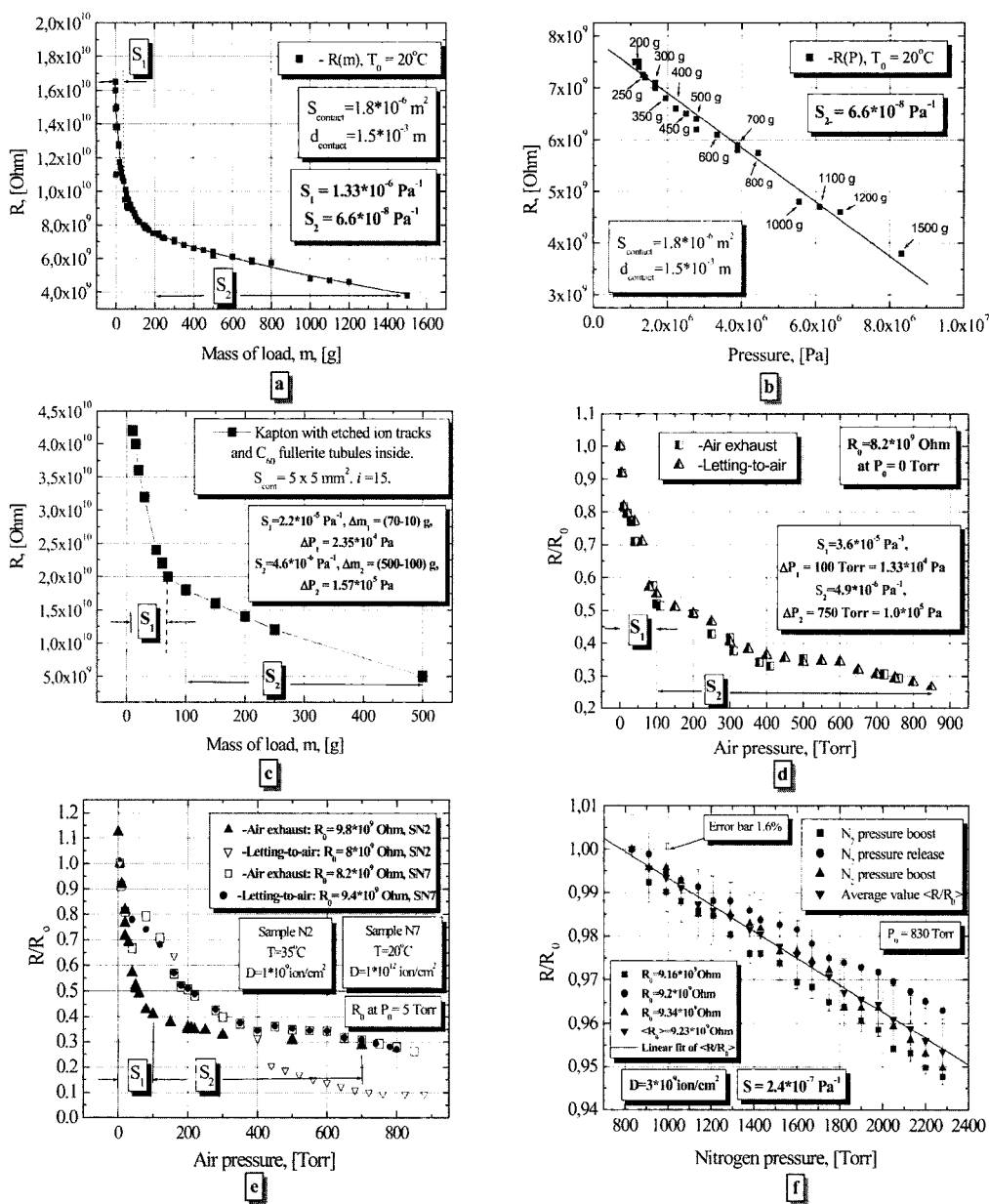


Fig. 5. $R(P)$ curves of fullerite in different configurations. a) C_{60}/C_{70} (85:15) powder, unidirectional compression, full curve, Fig. 1a, b) C_{60}/C_{70} (85:15) powder, unidirectional compression, high pressure branch, Fig. 1a, c) Thick C_{60} tubules in polyimide, unidirectional compression, Fig. 1b, d) Thin C_{60} tubules, isotropic compression, Fig. 1c, e) Si- C_{60} -Au planar structures, isotropic compression in air, (samples SN2; SN7), Fig. 1e, f) Si- C_{60} -Au planar structures, isotropic compression in nitrogen, (sample SN6), Fig. 1e.

5a) the low pressure branch has to be attributed largely to the rearrangement of the fullerite grains towards the geometrically most favorable distribution (i.e. reduction of the pore volume between the grains, Fig. 6a, whereas

the high pressure branch appears probably due to the reduction of the intermolecular distance of the fullerene molecules, Fig. 6b). Table 1 summarizes all experimentally measured results for different arrangements of sam-

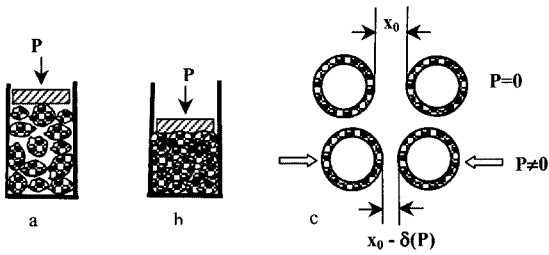


Fig. 6. Schematic sketch of C_{60} powder composition; a) at low pressure, b) at high pressure, and c) reduction of intermolecular distance by applied pressure.

ples according to Fig. 1. For the sake of easy comparison, also the dimensions, pressure range, resistance, resistivity and pressure sensitivity of the samples are given.

The values of bulk and surface resistivity, ρ_{bulk} ; $\rho_{surface}$, have been roughly estimated by the ordinary expressions: $R = \rho_{bulk} \cdot \frac{L_{cont}}{h_{layer} \cdot w_{cont}}$, $R = \rho_{surface} \cdot \frac{L_{cont}}{w_{cont}}$, where L_{cont} and w_{cont} are the distance between contacts and the width of contact, respectively. The corresponding values of low-pressure-branch sensitivity, S_1 , and high-pressure-branch sensitivity, S_2 , are given in Table

Table 1. The experimental date of pressure dependence of resistance for different arrangements of samples. $\langle S \rangle$ is of the average value of sensitivity.

| Structural arrangement | Dimensions | Pressure range and direction | Resistance, Resistivity, Pressure sensitivity |
|---|--|--|---|
| Fullerite powder in glass capillaries, Fig. 1a. | 0.75 and 1.5 mm \varnothing , ~0.5 mm length 30 nm C_{60} grains, $S_{cont}=1.8 \cdot 10^{-6} \text{ m}^2$ | ((0+1.5 kg)·9.8 m/s ²)/1.8·10 ⁻⁶ m ² 0+8.2·10 ⁶ Pa 0+3.27·10 ⁵ Pa 1.2·10 ⁶ +8.2·10 ⁶ Pa Unidirectional | 1.6·10 ¹⁰ +4·10 ⁹ Ω $\rho_{bulk}=5.76 \cdot 10^7 \pm 1.44 \cdot 10^7 \Omega \cdot \text{cm}$ $S_1=1.33 \cdot 10^{-6} \text{ Pa}^{-1}$ $S_2=6.6 \cdot 10^{-8} \text{ Pa}^{-1}$ |
| Fullerite tubules in etched tracks in polyimide foils, Fig. 1b. | 0.2 to 5 μm \varnothing , 10–25 μm length ~0.5 μm wall thickness ~3·10 ⁶ tubules/cm ² $S_{cont}=25 \cdot 10^{-6} \text{ m}^2$ | ((0+0.5 kg)·9.8 m/s ²)/25·10 ⁻⁶ m ² 0+1.96·10 ⁵ Pa 3.92·10 ³ +2.74·10 ⁴ Pa 3.92·10 ⁴ +1.96·10 ⁵ Pa Unidirectional | 4.3·10 ¹⁰ +5·10 ⁹ Ω $\rho_{bulk}=8 \cdot 10^{11} \pm 9.3 \cdot 10^{10} \Omega \cdot \text{cm}$ $S_1=2.2 \cdot 10^{-5} \text{ Pa}^{-1}$ $S_2=4.6 \cdot 10^{-6} \text{ Pa}^{-1}$ |
| Fullerite tubules in etched tracks in polyimide foils, Fig. 1c. | $S_{cont} \approx 3.14 \cdot 10^{-6} \text{ m}^2$ | 0+850 Torr, 0+1.13·10 ⁵ Pa 0+1.33·10 ⁴ Pa 1.33·10 ⁴ +1.13·10 ⁵ Pa Isotropic | 8.2·10 ⁹ +2.17·10 ⁹ Ω $\rho_{bulk}=1.85 \cdot 10^{10} \pm 0.5 \cdot 10^{10} \Omega \cdot \text{cm}$ $S_1=3.6 \cdot 10^{-5} \text{ Pa}^{-1}$ $S_2=4.9 \cdot 10^{-6} \text{ Pa}^{-1}$ |
| Si-p/ C_{60} /Au sandwich structure with intermittent Au films, Fig. 1e. Pristine or ion-irradiated 300 MeV $^{84}\text{Kr}^{14+}$, 0...1·10 ⁹ ...1·10 ¹² cm ⁻² . | $h_{Au}=50 \text{ \AA}$ $h_{fullerite}=2500 \text{ \AA}$ $h_{Si}=500 \text{ \mu m}$ $L_{cont} \approx 5 \text{ mm}$ $w_{cont} \approx 1 \text{ mm}$ | “SN2” 5+880 Torr, air “SN2” 6.66·10 ² +1.17·10 ⁵ Pa “SN2” 6.66·10 ² +2.13·10 ⁴ Pa “SN2” 13·10 ⁴ +1.17·10 ⁵ Pa Isotropic | 9.8·10 ⁹ +9.2·10 ⁸ Ω $\rho_{bulk}=5 \cdot 10^4 \pm 4.1 \cdot 10^3 \Omega \cdot \text{cm}$ $\rho_{surf}=1.96 \cdot 10^9 \pm 1.84 \cdot 10^8 \Omega$ $\langle S_1 \rangle = 3.2 \cdot 10^{-5} \text{ Pa}^{-1}$ $\langle S_2 \rangle = 6.7 \cdot 10^{-6} \text{ Pa}^{-1}$ |
| Si-p/ C_{60} /Au sandwich structure with intermittent Au films, Fig. 1e. Pristine or ion-irradiated 300 MeV $^{84}\text{Kr}^{14+}$, 0...3·10 ⁹ cm ⁻² . | | “SN7” 5+800 Torr, air “SN7” 6.66·10 ² +1.07·10 ⁵ Pa “SN7” 6.66·10 ² +2.66·10 ⁴ Pa “SN7” 2.66·10 ⁴ +1.07·10 ⁵ Pa Isotropic | 9.4·10 ⁹ +2.5·10 ⁹ Ω $\rho_{bulk}=4.8 \cdot 10^4 \pm 1.3 \cdot 10^3 \Omega \cdot \text{cm}$ $\rho_{surf}=1.9 \cdot 10^9 \pm 0.5 \cdot 10^9 \Omega$ $\langle S_1 \rangle = 1.9 \cdot 10^{-5} \text{ Pa}^{-1}$ $\langle S_2 \rangle = 5.7 \cdot 10^{-6} \text{ Pa}^{-1}$ |
| | | 830+2300 Torr, N ₂ 1.1·10 ⁵ +3.06·10 ⁵ Pa Isotropic | $\langle 9.2 \cdot 10^9 + 8.8 \cdot 10^9 \rangle \Omega$ $\langle \rho_{bulk} \rangle = 4.7 \cdot 10^4 \pm 4.5 \cdot 10^3 \Omega \cdot \text{cm}$ $\langle \rho_{surf} \rangle = 1.8 \cdot 10^9 \pm 1.7 \cdot 10^9 \Omega$ $\langle S \rangle = 2.4 \cdot 10^{-7} \text{ Pa}^{-1}$ |

1. Similarly, the inter-granular distance of the individual crystallites of the fullerite films in the arrangements according to Fig. 1b, c, and e is expected to be reduced by the applied pressure, and the naturally abundant pores will be compressed. These structural rearrangements should be independent of the way how the pressure is applied (this may be unidirectional or isotropic) and in fact our experiments show that in both cases the fullerite resistivity responds well to the pressure variations.

As in previous work^[8,11] fullerite was also found to be humidity sensitive than strong dependence $R(P)$ at low pressure branch for devices were shown by Fig. 1c, 1e (corresponding views are in Fig. 5d, 5e should be partly concerned with loss of moisture as a result of pumping-out process. To check influence of humidity the experiment with pumping-in of dry nitrogen was made. We have found remarkable differences in the pressure dependence of the fullerite resistivity when comparing dry nitrogen gas and ambient air (see Fig. 5f). Though more detailed examinations are still missing in this case, we tend to assume that the observed differences essentially relate to the differences in humidity. We supposed also that in the case of abundant pressure of nitrogen fullerite microcrystallines had been compressed enough, i.e. the pressure range corresponds to linear part of $R(P)$ dependence. The using of dry nitrogen allowed estimate factor of pressure sensitivity without any influence of humidity: $\langle S \rangle = 2.4 \cdot 10^{-7} \text{ Pa}^{-1}$. Some of the performed experiments show a hysteresis, but the deviations in resistance for pressure rise and release were always small and never exceeded 10%. Also the experiments with the Si-C₆₀-Au films (Fig. 5d) which probe essentially the pressure dependence of the surface resistance had been interpreted by the tendency to form more ordered crystal structures upon application of low pressure and by the reduction of the C₆₀ intermolecular distance in the high-pressure branch. Radiation damage destroys the ordered arrangement, which leads to a shifting of the $R(P)$ curves.

4. Conclusion

Fullerite powder, tubules or thin films can be used as sensitive material to probe unidirectional mechanical stress and isotropically applied pressure by the changes in its resistance. Fullerite can either be deposited by pre-

cipitation from a saturated solution of fullerene in toluene or it can be evaporated onto the corresponding surface, or one just can use fullerite powder. The sensitivity factor of fullerite-based pressure-sensors (FPS) is $\sim 10^{-5} - 10^{-8} \text{ 1/Pa}$, and thus comparable with the sensitivity factor of well-known silicon pressure sensors. However, the small sizes and simple production technology of FPS's opens challenging perspectives for creating a new family of cheaper sensors, and even of cheap two-dimensional high-resolution sensor fields. As good pressure sensitivity was found from pre-vacuum to at least atmospheric pressure. FPS's can also be applied as vacuum manometers.

Acknowledgments

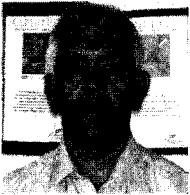
This project was enabled by the Grant T02-02.2-1576 Ministry of Education of Russian Federation and the Strategiefonds "Ion-Festkörper-Wechselwirkung" of the Helmholtz-Gesellschaft. We are grateful to the crew of the IBL accelerator (HMI-Berlin) for providing the ion irradiation of our base material. A.B. is obliged to the HMI and NSTU for research grants that enabled this work. We thank Mr. P. Zimkoviak (HMI-Berlin) for technical assistance. This work was supported in part by supported by 2003 Research Fund of University of Ulsan and the Korea Science and Engineering Foundation (KOSEF) through the Research Center for Machine Parts and Materials Processing (ReMM) at the University of Ulsan, Korea.

References

- [1] Dresselhaus M. S., Dresselhaus G., and Saito R. "Nanotechnology in carbon materials/nanotechnology, edited by gregory timp", *Springer-Verlag New-York Inc.*, pp. 285-329, 1999
- [2] Osip'yan Yu. A., Fortov V. E., Kagan K. L., Kveder V. V., Kulakov V. I., Kur'yanchik A. N., Nikolaev R. K., Postnov V. I., and Sidorov N. S., "Conductivity of C₆₀ fullerene crystals under dynamic compression up to 200 kbar", *JETP Letters*, vol. 75, no. 11, pp. 563-565, 2002.
- [3] Duclos S. J., Brister K., Haddon R. C., Kortan A. R., and Thiel F. A., "Effects of pressure and stress on C₆₀ fullerite to 20 GPa", *Nature*, vol. 351 pp. 380, 1991.
- [4] Hongkun Park, Jiwoong Park, Andrew K. L. Lim,

- Erik H. Anderson, Paul Alivisatos, and Paul L. McEuen, "Nanomechanical oscillations in a single C_{60} transistor", *Nature*, vol. 407, no. 7, pp. 57-60, September 2000.
- [5] S. Wen, J. Li, K. Kitazawa, T. Aida, I. Honma, H. Komiyama, and K. Yamada, "Electrical conductivity of a pure C_{60} single crystal", *Appl. Phys. Lett.* vol. 61, no. 18, pp. 2162-2163, 1992.
- [6] J. Mort, R. Ziolo, M. Machonkin, D. R. Huffman, and M. I. Ferguson, "Electrical conductivity studies of undoped solid films of C_{60}/C_{70} ", *Chem. Phys. Lett.*, vol. 186, pp. 281-283, 1991.
- [7] E. A. Katz, "Fullerene-based thin films as a novel polycrystalline semiconductor", *Solid State Phenomena*, vol. 67-68, pp. 435-446, 1999.
- [8] A. S. Berdinsky, Y. V. Shevtsov, A. V. Okotrub, S. V. Trubin, L. T. Chadderton, D. Fink, and J. H. Lee, "Sensor properties of fullerene films and fullerene compounds with iodine", *Chemistry for Sustainable Development*, vol. 8, pp. 141-146, 2000.
- [9] Berdinsky A. S. "Fullerite films new material for sensor electronics", *4th Siberian Russian Workshop and Tutorials EDM'2003*, Erlagol, pp. 1018, 2003.
- [10] E. A. Katz, D. Faiman, S. Goren, S. Shtutina, B. Mishori, and Yoram Shapira, "A photovoltaic C_{60} heterojunction", *Fullerene Science and Technology*, vol. 6, no. 1, pp. 103-111, 1998.
- [11] A. S. Berdinsky, Yu. V. Shevtsov, A. V. Okotrub, L. T. Chadderton, and A. M. Loganikhin, "Humidity-sensitive resistive sensors from C_{60} films", *International Symposium on Carbon, Science and Technology of New Carbons*, Tokyo, Tanzo, pp. 540-541, 1998.
- [12] Berdinsky A. S., Fink D., Petrov A. V., Müller M., Chadderton L. T., Chubaci J. F., and Tabacniks M. H. "Formation and conductive properties of miniaturized fullerite sensors", *MRS Fall Meeting*, November 26-30 in Boston, Massachusetts, Boston, USA, paper Y4.7, 2001.
- [13] J. Vacik, J. Cervena, V. Hnatowicz, D. Fink, and R. Klett, "New technique for nondestructing examination of latent track etching", *Rad. Eff. Def. Solids*, vol. 140, pp. 307-311, 1997.

Alexander S. Berdinsky



- born in 1946
- Ph.D from Novosibirsk State Technical Univ., 1976
- 2003.9 ~ Research professor in Opto-electronic Materials and Devices Lab., SunKyunKwan Univ., Korea
- Area of research : application of fullerene and carbon nanotubes for devices and sensors

Hui-Gon Chun

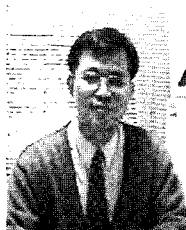
- J. of Korean Sensors Society Vol. 6. No. 1 p. 34

Dietmar Fink



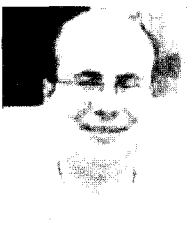
- born in 1943
- Ph.D from Free Univ. Berlin, 1974
- 1967 ~ Hahn-Meitner-Inst. Berlin
- Area of research : Ion Implantation, radiation damage, nuclear tracks

Ji-Beom Yoo



- born in 1959
- Ph.D from Stanford Univ., 1989
- Prof., Dept. of Materials Engineering, SungKyunKwan Univ., Korea
- Area of research : carbon nanotubes, nanostructure materials and its application

Alexander V. Petrov



- born in 1967
- Ph.D from Hahn-Meitner-Inst. Berlin
- Area of research : defect structure in metal, Ion Implantation, polymers, nuclear

Prashant S. Alegaonkar



- born in 1977
- Ph.D student at Univ. of Pune, India, 1999
- 1999 ~ Senior Research Fellow
- Dept. of Physics, Univ. of Pune, India
- Area of research : radiation damage, elemental diffusion in polyimide